Syntheses, structures, electrochemistry and magnetic properties of chain-like dicyanamide manganese(III) and iron(III) complexes with salen ligand

Qian Shi,[ab] Rong Cao,*[a] Xing Li,[a] Junhua Luo,[a] Maochun Hong*[a] and Zhongning Chen[a]

[a] *State Key Laboratory of Structural Chemistry, Fujian Institute of Research on the Structure of Matter, The Chinese Academy of Sciences, Fuzhou 350002, P. R. China. E-mail: hmc@ms.fjirsm.ac.cn*

[b] *Department of Chemistry, Wenzhou Teachers College, Wenzhou 325000, P. R. China*

Received (in Montpellier, France) 24th January 2002, Accepted 3rd May 2002
First published as an Advance Article on the web 21st August 2002

Two dicyanamide (dca) M^{III} complexes with salen ligand, $[Mn^{III}(salen)(dca)]_n$ (**1**) and $[Fe^{III}(salen)(dca)]_n$ (**2**), were synthesized and characterized. X-Ray diffraction analyses revealed the two complexes have a similar one-dimensional zig-zag chain structure constructed by $\mu_{1,5}$-dca bridge. Magnetic susceptibility measurements indicate the presence of antiferromagnetic interactions between two intra-chain high-spin Mn^{III} ions and between two intra-chain low-spin Fe^{III} ions *via* the dca bridge. The electrochemical properties of the two complexes were studied by cyclic voltammetry.

Dicyanamide (dca) bridged polynuclear transition metal complexes constitute a hot subject of research, due to their rich structural and topological features along with the magnetic properties related to this ligand. Surprisingly, most of the reported dca bridged transition metal complexes have focused on low-oxidation state systems such as M^{I} and M^{II}. For instances, the reactions of M^{I} (M = Cu, Ag) with dca yielded a series of discrete or polymeric structures;[1–3] the reactions of M^{II} with dca resulted in a great number of interesting structures, which usually possess the formulas $M^{II}(dca)_2$ or $M^{II}(dca)_2L$ (M = Cu, Co, Ni, Mn, Zn or Fe, L = co-ligand)[4–9] and show 0 to 3-D dimensional structures. To date, the high-oxidation state transition metal dca complexes, such as M^{III} or M^{IV} complexes, have been almost neglected.[10] As is well-known, six-coordinate manganese(III) and iron(III) Schiff base complexes display interesting structural and electronic effects;[11–13] the variation of in-plane chelating and axial sites often leads to a change in the spin state of the metal ions: high-spin, low-spin or spin-crossover state.[14–16] Accordingly, introducing a dca ligand into these M^{III}-Schiff base (M = Fe, Mn) systems will combine their interesting characteristics and result in the formation of M^{III}-dca complexes along with a rich coordination chemistry. In this work, salen anion [$salen^{2-}$ = *N*,*N*'-ethylenebis(salicylaldiiminato)] was selected as the Schiff base ligand, because upon deprotonation of the two hydroxyl groups it usually acts as a dianionic tetradentate ligand coordinating to a M^{III} ion, and the two remaining coordination sites of M^{III} are easily accessible to dca ligands to generate one-dimensional complexes with a single end-to-end dca bridge. This paper will report details of the syntheses and characterizations of two one-dimensional complexes, $[Mn(salen)(dca)]_n$ (**1**) and $[Fe(salen)(dca)]_n$ (**2**).

Experimental

Syntheses

$[Mn(salen)(dca)]_n$ 1. To a mixture of $Mn(OAc)_2{\cdot}4H_2O$ (492 mg, 2 mmol) and salicylaldehyde (540 mg, 4 mmol) in methanol (30 mL) was added 120 mg of ethylenediamine (2 mmol). After stirring at 60 °C for 0.5 h, the solution color changed from yellow to brown; a methanol solution (10 mL) of Na(dca) (180 mg, 2 mmol) was added dropwise into the mixture. After the solution stood at room temperature for 3 days, dark brown cubic crystals were obtained and washed with diethyl ether, yield 69%. Found (calcd) % for $C_{18}H_{14}MnN_5O_2$: C, 55.8 (55.8); H, 3.5 (3.6); N, 18.2 (18.1). IR (KBr, cm^{-1}): $[N(CN)_2]^-$, ν_s(C≡N) 2170(s), ν_{as}(C≡N) 2227(s), ν_s(C–N) 904(s), ν_{as}(C–N) 1292(s); ν(C=N) 1622(s), ν(Mn–N) 467(s), ν(Mn–O) 386(s).

$[Fe(salen)(dca)]_n$ 2. To a mixture of $FeCl_3{\cdot}6H_2O$ (320 mg, 2 mmol) and salicylaldehyde (540 mg, 4 mmol) in methanol (30 mL) was added 120 mg of ethylenediamine (2 mmol). After stirring at 60 °C for 0.5 h, an ethanol solution (10 mL) of Na(dca) (180 mg, 2 mmol) was added dropwise into the mixture. Red-brown cubic crystals along with a great-amount of red powder were obtained after 5 days. The red powder may be a mixture of by-products and efforts to characterize it were unsuccessful. The cubic crystals were separated manually and washed with diethyl ether, yield 33%; Found (calcd) % for $C_{18}H_{14}FeN_5O_2$: C, 55.6 (55.7); H, 3.6 (3.6); N, 18.1 (18.0). IR (KBr, cm^{-1}): $[N(CN)_2]^-$, ν_s(C≡N) 2177(s), ν_{as}(C≡N) 2245(s), ν_s(C–N) 906(s), ν_{as}(C–N) 1294(s); ν(C=N) 1626(s), ν(Mn–N) 432(s), ν(Mn–O) 382(s).

Physical measurements

Elemental analyses were determined on an Elementar Vario ELIII elemental analyzer. IR spectra were measured as KBr pellets on a Nicolet Magna 750 FT-IR spectrometer in the range of 200–4000 cm^{-1}. UV-visible spectra were recorded on a Lambda 35 spectrometer. ESR spectra were recorded as powder samples at the X-band frequency on a Bruker ER420 spectrometer at room temperature. The temperature-dependent magnetic measurements were determined in the temperature range 300–4 K on a SQUID magnetometer in an external field of 10 kG. Cyclic voltammetry was performed

This journal is © The Royal Society of Chemistry and the Centre National de la Recherche Scientifique 2002

on a PE-236A potentiostat with a three-electrode cell under an inert atmosphere, consisting of a platinum wire working electrode, Ag–AgCl reference electrode and a platinum auxiliary electrode; 0.1 mol·dm^{-3} [NBu$^n_4$][PF$_6$] was used as supporting electrolyte and the scan rate was 0.1 V s^{-1}.

Crystallographic measurements

X-Ray intensities of **1** and **2** were collected on a Siemens Smart CCD diffractometer with graphite-monochromated Mo-Kα radiation ($\lambda = 0.71073$ Å) with the $\omega - 2\theta$ scan mode. Empirical absorption correction was applied to the data using SADABS program.[17] The structures were solved by direct methods.[18] Non-hydrogen atoms were refined anisotropically. In the two complexes, the C(10) atom was treated with disorder in two positions [C(10A) and C(10B)], and the hydrogen atoms on the C(10A), C(10B) and C(11) atoms were generated from successive difference Fourier syntheses, while the other hydrogen atoms were generated in idealized positions. All calculations were performed using the SHELXTL program.[19] The crystallographic data and other pertinent information are summarized in Table 1 and the selected bond lengths and angles for the two complexes are given in Table 2.

CCDC reference numbers 178127 and 178128. See http://www.rsc.org/suppdata/nj/b2/b200907b/ for crystallographic files in CIF or other electronic format.

Results and discussion

Synthesis

In the preparation of complex **1**, Mn^{II} was oxidized to Mn^{III} by air under basic conditions during the synthetic reaction[11] and pure product with a composition of [Mn(salen)(dca)] was isolated in high yield. In the preparation of complex **2**, large quantities of by-products were observed, indicating that there might be different species in the reaction mixture. The formation of the isolated complexes can be understood from the solution behavior of the simple salen-M^{III} (M = Mn, Fe) complexes.[20–23]

Owing to the rich coordination mode of dca (*e.g.*, mono-, di- or tridentate) and the presence of an equilibrium between monomer and dimer of the salen-M^{III} complex, the addition of the dca ligand into the salen-M^{III} system may induce products with different configurations. In our experiment, complex **1** composed of a monomer unit is the major product isolated from the synthetic reaction, which may be attributed to the low solubility of **1** in common solvents such as MeOH, EtOH and MeCN. Upon formation **1** is easily deposited in crystalline form from the reaction mixture, resulting in a high yield of **1**. Interestingly, the synthetic reaction of **2** is much more complicated, and the solvent used in the reaction plays a crucial role in the formation of different products. If the reaction is carried out in a single solvent such as methanol, ethanol or acetonitrile, the major product is [Fe(salen)Cl], as confirmed by elemental analysis and IR spectrum. Complex **2** can only be successfully isolated in a mixed solvent, MeOH–EtOH. Although the reason why dca does not coordinate to the Fe^{III}-salen complex in single solvent systems is still unclear, the difficult synthesis of **2** may be caused by its high solubility in solvents such as MeOH or CH_3CN. Thus, during the reaction many Fe(salen)(dca) species, which may change conformation as shown by the CV determination (see below), may be present in the solution leading to a complex system and rendering the synthesis of **2** more difficult. Using the MeOH–EtOH mixed solvent may change the polarity of the solvent and lower the solubility of **2**, allowing the successful precipitation of **2** in crystalline form from the solution.

Table 1 Crystallographic data for **1** and **2**

	1	**2**
Empirical formula	$C_{18}H_{14}MnN_5O_2$	$C_{18}H_{14}FeN_5O_2$
Formula weight	387.28	388.19
T/K	293(2)	293(2)
Wavelength/Å	0.71073	0.71073
Crystal system	Orthorhombic	Orthorhombic
Space group	*Pbca*	*Pbca*
a/Å	11.2826(1)	11.4946(3)
b/Å	17.0485(2)	16.5213(4)
c/Å	17.5949(3)	17.8642(1)
μ/Å^3	3384.40(8)	3392.51(12)
Z	8	8
μ/mm^{-1}	0.803	0.912
Reflections collected	10 087	10 389
Independent reflections	2983	2989
R_{int}	0.0405	0.0684
$R_1[I > 2\sigma(I)]$	0.0446	0.0530
wR_2 (all data)	0.1079	0.1264

Table 2 Selected bond distances (Å) and angles (°) for **1** and **2**[a]

Complex **1**			
Mn–O(1)	1.882(2)	Mn–O(2)	1.882(2)
Mn–N(4)	1.983(3)	Mn–N(5)	1.986(3)
Mn–N(1)	2.304(3)	Mn–N(3A)	2.317(3)
O(1)–Mn–O(2)	95.46(19)	O(1)–Mn–N(4)	91.31(11)
O(2)–Mn–N(4)	173.22(11)	O(1)–Mn–N(5)	173.10(10)
O(2)–Mn–N(5)	91.43(10)	N(4)–Mn–N(5)	81.80(12)
O(1)–Mn–N(1)	91.26(11)	O(2)–Mn–N(1)	90.47(11)
N(4)–Mn–N(1)	89.03(12)	N(5)–Mn–N(1)	88.93(11)
O(1)–Mn–N(3A)	91.84(10)	O(2)–Mn–N(3A)	91.60(11)
N(4)–Mn–N(3A)	88.53(12)	N(5)–Mn–N(3A)	87.71(11)
N(1)–Mn–N(3A)	176.10(11)		
Complex **2**			
Fe–O(1)	1.892(3)	Fe–O(2)	1.892(3)
Fe–N(4)	2.105(4)	Fe–N(5)	2.107(4)
Fe–N(1)	2.157(4)	Fe–N(3A)	2.171(4)
O(1)–Fe–O(2)	105.81(13)	O(1)–Fe–N(4)	88.40(15)
O(2)–Fe–N(4)	165.63(15)	O(1)–Fe–N(5)	165.98(14)
O(2)–Fe–N(5)	88.21(14)	N(4)–Fe–N(5)	77.58(16)
O(1)–Fe–N(1)	92.20(14)	O(2)–Fe–N(1)	93.37(14)
N(4)–Fe–N(1)	88.10(16)	N(5)–Fe–N(1)	86.95(15)
O(1)–Fe–N(3A)	92.29(14)	O(2)–Fe–N(3A)	90.83(14)
N(4)–Fe–N(3A)	86.39(16)	N(5)–Fe–N(3A)	87.33(15)
N(1)–Fe–N(3A)	172.19(16)		

[a] Symmetry code A: $-x+3/2, y-1/2, z$ for **1** and $-x+1/2, y-1/2, z$ for **2**.

Electronic spectra

The electronic spectra of the two complexes in MeOH were recorded in the range of 200–800 nm, as shown in Fig. 1. The intense absorption bands at short wavelengths, 202 ($\varepsilon = 5900$ dm^3 mol^{-1} cm^{-1}) and 241 nm ($\varepsilon = 3077$ dm^3 mol^{-1} cm^{-1}) for complex **1**, 204 ($\varepsilon = 5900$ dm^3 mol^{-1} cm^{-1}) and 234 nm ($\varepsilon = 4336$ dm^3 mol^{-1} cm^{-1}) for complex **2**, may be assigned to intraligand π-π^* transitions in the complexes.[24] The absorptions at 282 nm ($\varepsilon = 1349$ dm^3 mol^{-1} cm^{-1}) for complex **1** and 320 nm ($\varepsilon = 1035$ dm^3 mol^{-1} cm^{-1}) for complex **2** may be assigned to a Schiff base to metal ion charge-transfer band (LMCT).[23]

Crystal structures

Complex **1** possesses a one-dimensional zig-zag chain structure, which is constructed by square-planar Mn^{III}-salen species (the average deviation is 0.005 Å) bridged by dca ligands in an anti-anti configuration, as shown in Fig. 2(A). The Mn^{III} ion is

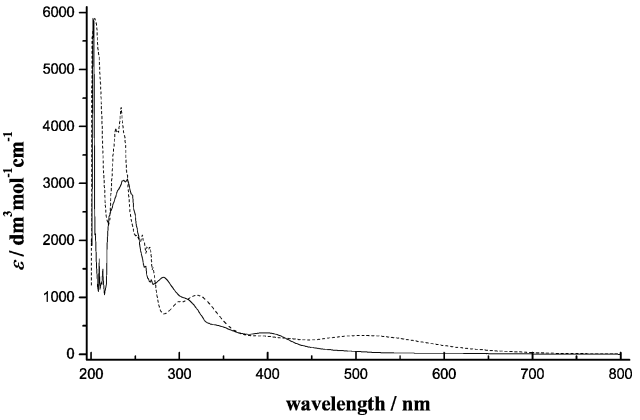

Fig. 1 UV-Vis absorption spectra of $[Mn(salen)(dca)]_n$ (solid line) and $[Fe(salen)(dca)]_n$ (dashed line) in MeOH.

in a slightly distorted octahedral geometry where the donor atoms from the salen ligand [O(1), O(2), N(4) and N(5)] form the equatorial plane with the angles subtended at the Mn^{III} ion varying from 81.80(12)° to 95.46(9)° (see Table 2), and the two nitrogen atoms from different dca ligands [N(1) and N(3A)] occupy the axial positions with the N(1)–Mn–N(3A) angle being 176.10(11)°. The in-plane bond distances of Mn–O [1.882(2) Å] and Mn–N [1.983(3) and 1.986(3) Å] show typical values for a high-spin Mn^{III} ion.[25,26] The axial Mn–N(dca) bond lengths [2.304(3) and 2.317(3) Å] are significant longer than the corresponding values in salen-Mn^{III} complexes {such as 2.25(3) Å in $[Mn(salen)CN]_n$,[14] 2.278(5) Å in {Mn[1,4-di(1-inidazolyl)butane](salen)},[27] 2.162(7) Å in [Mn(salen)(NCS)][25]}, and also much longer than the Mn–N(dca) bond lengths in $[Mn^{II}(\mu_{1,5}\text{-dca})(NO_3)(terpy)]_n$ [2.196(3) and 2.218(3) Å] and $[Mn^{II}(\mu_{1,5}\text{-dca})(H_2O)(terpy)]_n$ [2.162(2) and 2.182(2) Å].[8] This axial elongation may be attributed to a Jahn–Teller distortion, which is commonly observed in octahedral Mn^{III} complexes.[28]

Complex **2** is the isomorph of **1** with replacement of Mn^{III} by Fe^{III} [Fig. 2(B)]. However, the octahedral polyhedron around Fe^{III} is highly distorted as compared to that of Mn^{III}. The angles subtended at the Fe^{III} ion in the equatorial plane (the average deviation is 0.019 Å) formed by donor atoms from the salen ligand vary from 77.58(16)° to 105.81(13)°, and the

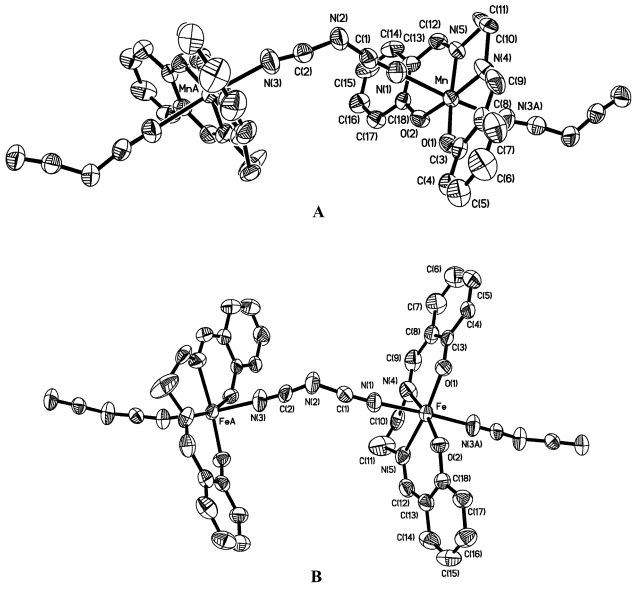

Fig. 2 ORTEP plots for the title complexes: (A) $[Mn(salen)(dca)]_n$, (B) $[Fe(salen)(dca)]_n$.

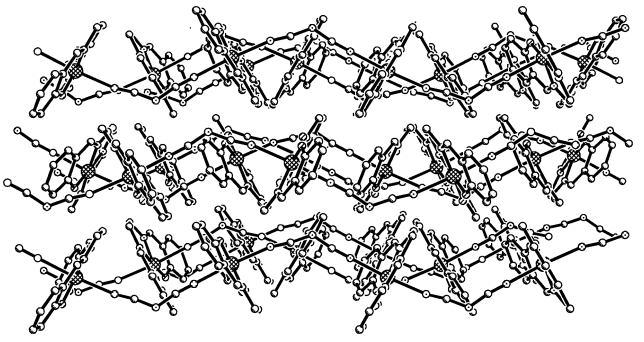

Fig. 3 Adjacent tightly packed chains in **2**.

bond N(1)–Fe–N(3A) angle is 172.19(16)°. The in-plane Fe–O and Fe–N bond lengths are 1.892(3), 1.892(3), 2.105(4) and 2.107(4) Å, respectively, similar to that in $[Fe^{III}(salen)(OAc)]_n$.[13] The axial Fe–N(dca) bond lengths [2.157(4) and 2.170(4) Å] are significantly shorter than the corresponding value of Mn–N(dca) in **1**, which may be due to different Jahn–Teller effects in octahedral Mn^{III} ($3d^4$) and Fe^{III} ($3d^5$) complexes. Interestingly, the inter-chain M–M distances in the two complexes (7.633 to 7.525 Å for **1** and 7.710 to 7.751 Å for **2**) are shorter than the corresponding intra-chain values (8.555 Å for **1** and 8.326 Å for **2**). Fig. 3 shows the adjacent tightly packed chains in **2**.

Magnetic properties

The plots of the molar magnetic susceptibility χ_M *versus* temperature T and the effective magnetic moment μ_{eff} *versus* T for complexes **1** and **2** are shown in Fig. 4.

For complex **1**, the μ_{eff} value of 4.70 μ_B at room temperature is slightly lower than the spin-only value for high-spin Mn^{III} (4.90 μ_B). On lowering the temperature, the μ_{eff} value decreases smoothly from 300 to 90 K, and then increases gradually from 90 to 22 K before abruptly reaching the minimum value of 4.23 μ_B at 5 K. This behavior indicates the presence of a weak antiferromagnetic interaction between two high-spin Mn^{III} ions *via* the dca bridge. The X-band ESR spectrum recorded on a powder sample prepared from the crystals at room temperature shows no signal, due to non-Kramer spin states ($S = 2$) of the Mn^{III} ion, as a result of either large zero-field splitting or fast relaxation processes.[24]

For complex **2**, the μ_{eff} value of 1.728 μ_B at room temperature is in agreement with the spin-only value for low-spin Fe^{III} (1.73 μ_B). The ESR spectrum of **2** recorded on a powder sample prepared from the crystals at room temperature shows a broad isotropic signal centered at $g = 2.0140$ (peak-to-peak line width 1833 G), confirming the low-spin state of the Fe^{III} ion in **2**.[29] On lowering the temperature, the μ_{eff} value decreases slowly to reach the minimum value of 1.15 μ_B at 5 K, indicating the presence of an antiferromagnetic interaction between two magnetic centers *via* the dca bridge.

The magnetic data of **1** and **2**, were analyzed by means of the analytical expression derived by Fisher:[30]

$$\chi_M = \frac{Ng^2\beta^2 S(S+1)}{3kT}\cdot\frac{1+u}{1-u} \qquad (1)$$

$$u = \coth\frac{JS(S+1)}{kT} - \frac{kT}{JS(S+1)}$$

for the magnetic susceptibility of an infinite chain of classical spins based on the Hamiltonian $H = -J\Sigma S_i S_{i+1}$ for local spin values $S = 2$ for Mn^{III} in **1** and $S = 1/2$ for Fe^{III} in **2**. The best fit parameters are: $J = -0.24$ cm^{-1}, $g = 1.99$, $R = 1.24 \times 10^{-6}$; $J = -7.65$ cm^{-1}, $g = 2.01$, $R = 4.01 \times 10^{-6}$ for **1** and **2**, respectively, where $R = \sum_{i=1}^{m}(\chi_i^{calc} - \chi_i^{exp})^2 / \sum_{i=1}^{m}(\chi_i^{exp})^2$.

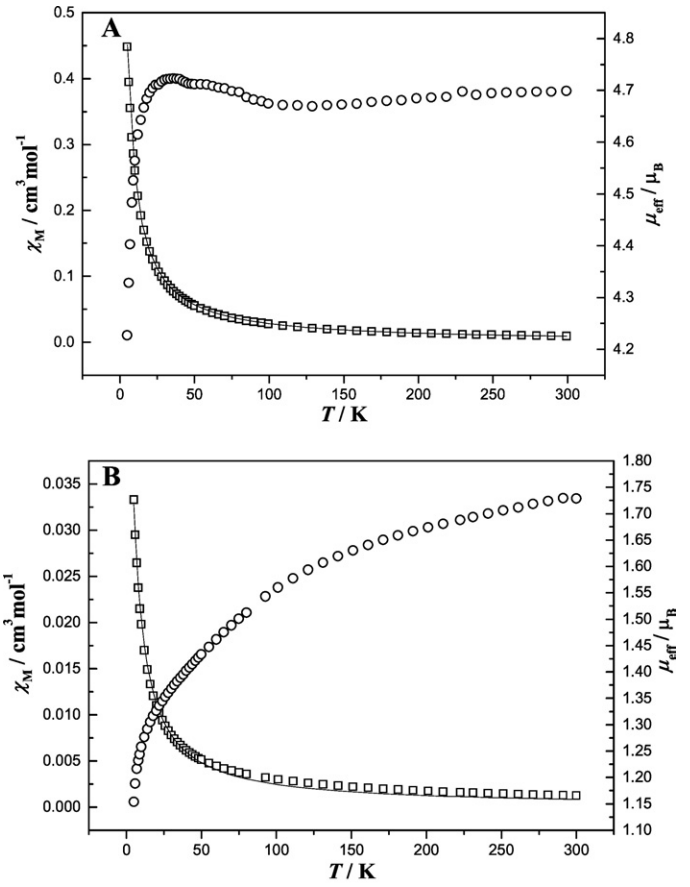

Fig. 4 Plots of χ_M *vs.* T (□) and μ_{eff} *vs.* T (○) for: (A) $[Mn(salen)(dca)]_n$, (B) $[Fe(salen)(dca)]_n$. The solid lines show the best fits to the model.

Cyclic voltammetry studies

The cyclic voltammogram of **1** was obtained in DMF solution (Fig. 5). Only one quasi-reversible redox couple at −0.274/−0.068 V is observed. This result indicates that only a single species of **1** is present in solution and the redox process may be assigned to the $[Mn^{III}(salen)(dca)] \leftrightarrow [Mn^{II}(salen)(dca)]^-$ reductive process.[11,31,32] Surprisingly, the cyclic voltammogram of **2** in DMF is rather complicated; several irreversible peaks (−1.546, 1.004 and 1.178 V) and a quasi-reversible couple (−0.396/−0.758 V) are observed. A detailed explanation remains unavailable as the redox behavior of **2** in DMF is very complicated different species accompanied by some irreversible chemical process may be present in DMF solution. This result is in agreement with those reported for $[Fe^{III}(salen)(ox)]^-$ which is also present as different species in DMF solution.[23] This lends support to our discussion on the formation of **2** (see above).

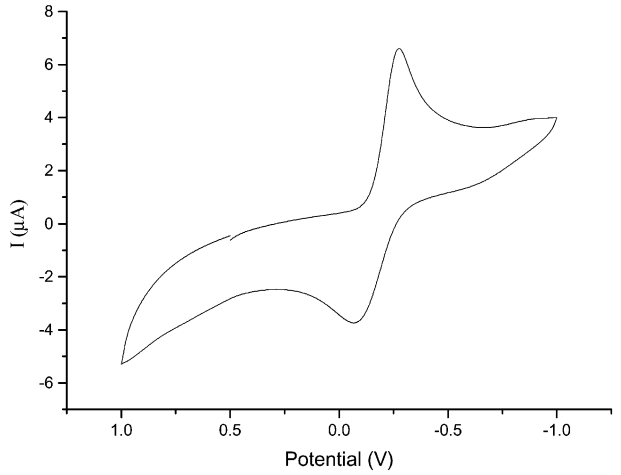

Fig. 5 Cyclic voltammogram of **1** in DMF.

Conclusion

We have successfully synthesized two one-dimensional zig-zag chain-like M^{III}-dca polymeric complexes with the salen ligand, $[Mn^{III}(salen)(dca)]_n$ (**1**) and $[Fe^{III}(salen)(dca)]_n$ (**2**). Magnetic susceptibility measurements indicate the presence of antiferromagnetic interactions between two intra-chain high-spin Mn^{III} ions in **1** and between two intra-chain low-spin Fe^{III} ions in **2** *via* the dca bridge. The cyclic voltammetry studies indicate that there is only a single species for **1** but there are several species for **2** in solution.

Acknowledgements

The authors thank for the financial support from NNSFC, Natural Foundation of Fujian Provice and the key project of CAS.

References

1 K. E. Bessier, L. L. Romualdo, V. M. Dellon and A. Hagenbach, *Z. Anorg. Allg. Chem.*, 2000, **626**, 1942.
2 D. Britton, *Acta Cryst. allogr., Sect. C*, 1990, **46**, 2297.
3 S. R. Batten, A. R. Harris, P. Jensen, K. S. Murray and A. Ziebell, *J. Chem. Soc., Dalton Trans.*, 2000, 3829.
4 P. Jensen, D. J. Price, S. R. Batten, B. Moubaraki and K. S. Murray, *Chem. Eur. J.*, 2000, **17**, 3186.
5 J. L. Manson, D. W. Lee, A. L. Rheingold and J. S. Miller, *Inorg. Chem.*, 1998, **37**, 5966.

6 I. Dasna, S. Golhen, L. Ouahab, O. Peña, J. Guillevic and M. Fettouhi, *J. Chem. Soc., Dalton Trans.*, 2000, 129.
7 S. Triki, F. Thétiot, J.-R. Galán-Mascarós, J. S. Pala and K. R. Dunbar, *New J. Chem.*, 2001, **25**, 954.
8 A. Claŕamunt, A. Escuer, F. A. Mautner, N. Sanz and R. Vicente, *J. Chem. Soc., Dalton Trans.*, 2000, 2627.
9 B.-W. Sun, S. Gao, B.-Q. Ma, D.-Z. Niu and Z.-M. Wang, *J. Chem. Soc., Dalton Trans.*, 2000, 4187.
10 H. Miyasaka, R. Clerac and C. S. Campoe-Fernandez, *Inorg. Chem.*, 2001, **40**, 1663.
11 M. Hirotsu, K. Nakajima, M. Kojima and Y. Yoshikawa, *Inorg. Chem.*, 1995, **34**, 6173.
12 C. E. Hulme, M. Watkinson, M. Haynes, R. G. Pritchard, C. A. McAuliffe, N. Jaiboon, B. Beagley, A. Sousa, M. R. Bermejo and M. Fondo, *J. Chem. Soc., Dalton Trans.*, 1997, 1805.
13 G. Liu, A. M. Arif, F. W. Bruenger and S. C. Miller, *Inorg. Chim. Acta*, 1999, **287**, 109.
14 N. Matsumoto, Y. Sunatsuki, H. Miyasaka, Y. Hashimoto, D. Luneau and J.-P. Tuchagues, *Angew. Chem., Int. Ed.*, 1999, **38**, 171.
15 H. Miyasaka, H. Ieda, N. Matsumoto, N. Re, R. Crescenzi and C. Floriani, *Inorg. Chem.*, 1998, **37**, 255.
16 N. Re, R. Crescenzi, C. Floriani, H. Miyasaka and N. Matsumoto, *Inorg. Chem.*, 1998, **37**, 2717.
17 G. M. Sheldrick, SADABS, Program for Empirical Absorption Correction of Area Detector Data, University of Göttingen, Germany, 1996.
18 G. M. Sheldrick, SHELXS 97, Program for Crystal Structure Solution, University of Göttingen, Germany, 1997.
19 G. M. Sheldrick, SHELXTL 97, Program for Crystal Structure Refinement, University of Göttingen, Germany, 1997.
20 H.-L. Shyu, H.-H. Wel and Y. Wang, *Inorg. Chim. Acta*, 1999, **290**, 8.
21 M. D. Hobday and T. C. Smith, *Coord. Chem. Rev.*, 1972, **9**, 311.
22 H. Miyasaka, N. Matsumoto, H. Ōkawa, N. Re, E. Gallo and C. Floriani, *J. Am. Chem. Soc.*, 1996, **118**, 981.
23 A. Geiß and H. Vahrenkamp, *Eur. J. Inorg. Chem.*, 1999, 1793.
24 X. S. Tan, J. Chen, Z. N. Chen, P. J. Zheng and W. X. Tang, *Inorg. Chim. Acta*, 1995, **234**, 27.
25 M. Mikuriya, Y. Yamato and T. Tokii, *Bull. Chem. Soc. Jpn.*, 1992, **65**, 1466.
26 M. Mikuriya, S. Kida and I. Murase, *Chem. Lett.*, 1988, 35.
27 N. Matsumoto, N. Takemoto, A. Ohyosi and H. Ōkawa, *Bull. Chem. Soc. Jpn.*, 1988, **61**, 2984.
28 F. A. Cotton, G. Wilkinson, C. A. Murillo and M. Bochmann, *Advanced Inorganic Chemistry*, John Wiley & Sons, 6th edn., 1999.
29 B. J. Kennedy, G. Brain, E. Horn, K. S. Murray and M. R. Snow, *Inorg. Chem.*, 1985, **24**, 1647.
30 M. E. Fisher, *Am. J. Phys.*, 1964, **32**, 343.
31 M. R. Bermejo, A. M. González, M. Fondo, A. García-Deibe, M. Maneiro, J. Sanmartín, O. L. Hoyos and M. Watkinson, *New. J. Chem.*, 2000, **24**, 235.
32 S.-B. Yu, C.-P. Wang, E. P. Day and R. H. Holm, *Inorg. Chem.*, 1991, **30**, 4067.